showed strong species-specific differences. It is unknown whether these compounds are involved in species recognition.

The above-mentioned volatile acids may form a less species-specific long-range pheromone that is embedded in a species-specific matrix that accounts for close-range recognition. In another linyphiid, *Frontinella pyramitela*, spiders are able to distinguish between sexes by use of chemical stimuli emitted from the cuticle (*17*).

REFERENCES AND NOTES

1. W. S. Bristowe and G. H. Locket, *Proc. Zool. Soc. London* **1926**, 317 (1926).
2. W. J. Tietjen and J. S. Rovner, *Chemical Communication: Mechanisms and Ecological Significance*, P. N. Witt and J. S. Rovner, Eds. (Princeton Univ. Press, Princeton, NJ, 1982), pp. 249–279.
3. P. J. van Helsdingen, *Zool. Meded. Rijks Nat. Hist. Leiden* **41**, 15 (1965); J. S. Rovner, *Z. Tierpsychol.* **25**, 232 (1968).
4. P. J. Watson, *Science* **233**, 219 (1986).
5. S. Toft and S. Schulz, unpublished data.
6. S. Toft, *Bull. Br. Arachnol. Soc.* **8**, 33 (1989).
7. We did not follow web reduction to completion in order to test several males on each web. Cutting of threads has been observed in one other context: males walking on the upper side of the female's sheet may cut a small hole through which they can get to the underside. Web reduction is always done from below the sheet. Cutting single threads is very rarely observed and has never been accepted as a positive response. Our 5-min criterion was chosen to allow the males to recover from the disturbance due to experimental manipulation and to allow for the variable time spent in zigzag walking. We knew from experience that web reduction rarely started later.
8. (*R*)-HBA was synthesized from poly-(*R*)-3-hydroxybutyrate by solvolysis with methanol followed by saponification [D. Seebach and M. Züger, *Helv. Chim. Acta* **65**, 495 (1982)]. (*S*)-HBA was obtained by yeast reduction of ethyl acetoacetate followed by saponification [E. Hungerbühler, D. Seebach, D. S. Wasmuth, *Helv. Chim. Acta* **64**, 1467 (1981)]. (*R,R*)-HBBA was prepared starting from (*R*)-HBA by protection of the alcohol or acid function, respectively, followed by condensation of the two units and deprotection [D. Seebach, U. Brändli, P. Schnurrenberger, *Helv. Chim. Acta* **71**, 155 (1988); T. Tanio *et al.*, *Eur. J. Biochem.* **124**, 71 (1982)].
9. W. A. König, R. Krebber, P. Mischnick, *J. High Resolut. Chromatogr.* **12**, 732 (1988).
10. D. Seebach, A. K. Beck, R. Breitschuh, K. Job, *Org. Synth.* **71**, 39 (1992).
11. Y. Doi, *Microbial Polyesters* (VCH, New York, 1990).
12. G. Kunesch, P. Zagatti, A. Pouvreau, R. Cassini, *Z. Naturforsch. Teil C* **42**, 657 (1987); J. M. Brand, J. W. Bracke, A. J. Markovetz, D. L. J. Wood, L. E. Brown, *Nature* **254**, 136 (1975).
13. If microorganisms are involved in the pheromone production, the spider must have a mechanism to stop them from producing HBBA.
14. S. Toft, *Oecologia (Berlin)* **72**, 216 (1987).
15. K. H. Lockey, *Comp. Biochem. Physiol. B* **89**, 595 (1988).
16. S. Schulz and S. Toft, *Tetrahedron*, in press.
17. R. B. Suter, C. M. Shane, A. J. Hirscheimer, *J. Arachnol.* **15**, 157 (1987).
18. In the experiments we used empty webs of mated females. Before spraying, a series of males was tested on each web to ascertain lack of activity (control columns). Subsequently the webs were sprayed with a methylene chloride solution of 1 to 5 mg of each compound, and the males were added again after evaporation of the solvent (test columns). Because of the open structure of the web, only a small amount of the solution was actually applied on the silk by the spraying procedure. Positive responses were obtained only during the first 30 to 60 min after spraying, indicating rapid evaporation or deactivation of the applied compound. The webs were therefore resprayed at regular intervals, which usually reactivated the web. As a result of the deactivation of the pheromone, the chances of a positive response decrease with time and positive responses are therefore underrated in the test. Rather than reducing the data set to results obtained within a restricted period of time after spraying, we have analyzed the full data set, as this made it more difficult for us to obtain statistical significance. However, because the controls showed no positive responses, the statistical significance is rather insensitive to variations in the male response rate. The statistical test we used is the χ^2 test. The response frequency of the males seemed to depend also on uncontrolled environmental factors such as barometric pressure and air humidity. Evaluation of these factors is in progress.

19. We thank S. Westermann for preliminary experiments, K. Rosendahl for technical assistance, W. Francke for critical review of the manuscript, W. A. König for supplying the Lipodex E GC column, and D. Seebach for additional samples of HBBA.

23 November 1992; accepted 14 April 1993

Structural Basis of Amino Acid α Helix Propensity

Michael Blaber, Xue-jun Zhang, Brian W. Matthews*

The propensity of an amino acid to form an α helix in a protein was determined by multiple amino substitutions at positions 44 and 131 in T4 lysozyme. These positions are solvent-exposed sites within the α helices that comprise, respectively, residues 39 to 50 and 126 to 134. Except for two acidic substitutions that may be involved in salt bridges, the changes in stability at the two sites agree well. The stability values also agree with those observed for corresponding amino acid substitutions in some model peptides. Thus, helix propensity values derived from model peptides can be applicable to proteins. Among the 20 naturally occurring amino acids, proline, glycine, and alanine each have a structurally unique feature that helps to explain their low or high helix propensities. For the remaining 17 amino acids, it appears that the side chain hydrophobic surface buried against the side of the helix contributes substantially to α helix propensity.

Estimates of the α helix propensity of the different amino acids have been made on the basis of many different sources including statistical surveys (*1, 2*), host-guest analysis (*3*), model peptides (*4–7*), directed mutagenesis (*8, 9*), and molecular dynamics calculations (*10, 11*). To determine α helix propensity in the context of a folded protein and to obtain insights into its underlying physical basis, we made multiple amino acid replacements at each of two positions in α helices of T4 lysozyme.

Ideally, the substitution site for such an experiment would be in the middle of a relatively long, regular helix and would be exposed to solvent, remote from charged groups, devoid of possible contacts with neighboring side chains, and not close to a contact site in the crystals. Because all of these criteria cannot be met in T4 lysozyme, Ser^{44} and Val^{131} were chosen as compromises (*12*). All 19 alternative amino acids were substituted at position 44 (*13*), and the proteins were purified (*14*). For 13 replacements (Ala, Arg, Asn, Glu, Gly, Ile, Leu, Lys, Phe, Pro, Thr, Trp, and Val), crystals suitable for structural analysis were obtained (*15*). The coordinates have been deposited in the Brookhaven Protein Data Bank.

Institute of Molecular Biology, Howard Hughes Medical Institute, and Department of Physics, University of Oregon, Eugene, OR 97403.

*To whom correspondence should be addessed.

With the exception of Pro, no substitution significantly distorted the α helix backbone. In the isomorphous structures (except for Pro) the backbone atoms within the α helix superimposed within 0.10 to 0.14 Å (Fig. 1A). For the nonisomorphous structures, the corresponding values were 0.19 to 0.33 Å but did not suggest a distortion of the helix (Fig. 1B). Thus, except for Pro there is no clear evidence that differences in helix propensity are caused by different amounts of strain introduced within the α helix. Similar structural results were observed for eight variants at position 131 (*16*).

We determined the thermostabilities of the mutant lysozymes (Table 1) by recording the circular dichroism as a function of temperature (*17*). Excluding those of Asp and Glu, the differences between the free energy of unfolding of each mutant and that of the Gly variant used for the site 131 replacements are remarkably similar to those at site 44 (correlation of 97%). In the crystal structure of the Asp^{131} variant, Asp^{131} forms a salt bridge with Arg^{154}, and we presume that electrostatic stabilization also occurs for Glu^{131}. The measured ΔΔG values were compared with other determinations of helix propensity (Table 1). The agreement with propensity scales that were derived from three studies of model peptides (*4–6*) was good (correlations of 71 to 93%), despite the different sequences involved, the differences

in the experimental systems, and the small span of energy values. Agreement with scales derived from the frequency of occurrence in protein structures (*1*, *2*) and from host-guest analysis (*3*) was also good (correlations of 81 and 69%, respectively).

The nature of the unfolded state of proteins has been controversial. Is the unfolded state random and fully solvated, or does it have sequence-dependent interactions that are influenced by mutations (*18*)? The agreement between T4 lysozyme and, for example, the model peptide of Lyu and colleagues (6) is good, although the $\Delta\Delta G$ values are relatively small. This correlation suggests that the unfolded state of T4 lysozyme is thermodynamically equivalent to that of the unfolded model peptide and is not significantly altered by substitutions at site 44 (or at site 131).

Within an α helix, the side chain atoms of one residue can contact the backbone (or side chain) atoms of residues in the next turn of the helix and may thereby be removed from contact with the solvent (*19*). For this reason it has long been expected that hydrophobic effects might contribute to differences in α helix propensity (*19*, *20*). As a test of this hypothesis, the observed $\Delta\Delta G$ values were plotted as a function of the hydrophobic surface area that is buried when residue 44 is transferred from a fully extended model peptide to the α helix, as observed in the available crystal structures (Fig. 2). The values for a subset of the 20 amino acids (Asn, Glu, Ser, Thr, Val, Lys, Ile, and Leu) fall approximately on a straight line, the slope of which is 19 kcal mol^{-1} $Å^{-2}$. The correspondence between this value and the commonly accepted range of 20 to 30 kcal mol^{-1} $Å^{-2}$ for hydrophobic stabilization (*21*) suggests that the hydrophobic effect is a major factor in the determination of the helix propensity of these amino acids. There are structural reasons why the values for other amino acids (Gly, Ala, Arg, Phe, and Trp) deviate substantially from the straight line (*22*).

For the remaining substitutions at site 44 for which crystal structures were not available, the buried surface areas were calculated on the assumption that the site 44 side chains were fully extended and that the protein structures were otherwise identical with the wild-type structure. Also in Fig. 2 are the observed values of $\Delta\Delta G$ (Table 1) and the calculated surface areas derived from the crystal structures of the substitutions made at site 131. Because of contributions from side chain entropy (*11*, *23*) and other factors, a perfect correlation is not expected between buried surface area and helix propensity. However, the approximately linear dependence of helix propensity on buried surface area, for many of the amino acids (Fig. 2), suggests that hydrophobic stabilization contributes substantially to helix propensity.

Our results show a good agreement between helix propensity determined in the context of a folded protein and that derived from studies of some helical peptides. At

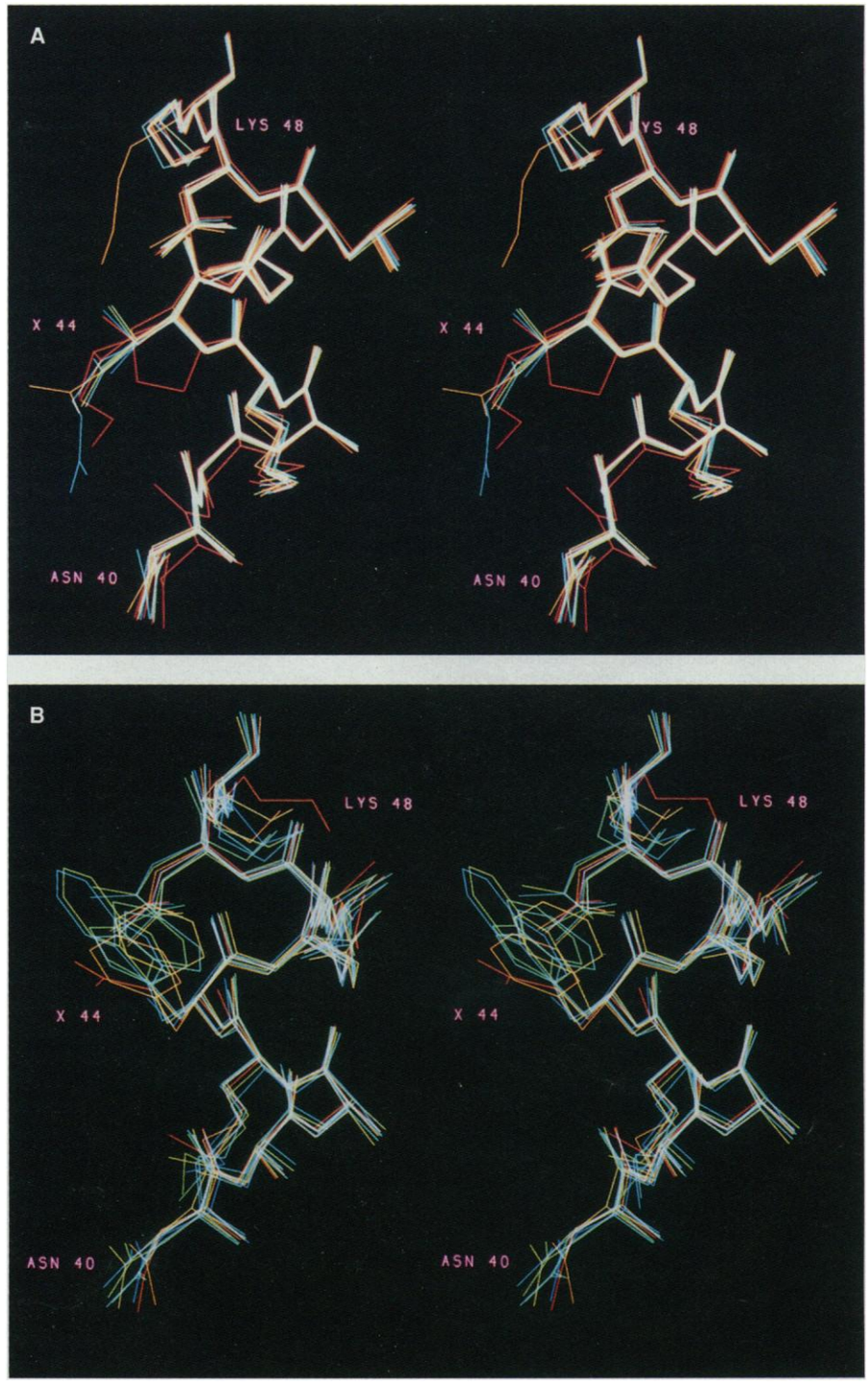

Fig. 1. (**A**) A stereodiagram of all the structures with replacements at position 44 that crystallized isomorphously with the wild type. Color scheme: Ala, orange; Asn, cyan; Arg, light blue; Glu, yellow; Gly, chartreuse; Ile, light green; Leu, red; Lys, red; Pro, red; Ser (wild type), red; Thr, blue; Val, green. The structures were aligned on the basis of least-squares superposition of the backbone atoms of residues 40 to 49. (**B**) A stereodiagram of the position 44 variants that crystallized in nonisomorphous forms. Included are two distinct forms of the Phe^{44} variant (yellow and chartreuse), four distinct forms of the Trp^{44} variant (light green, green, cyan, and light blue), the Glu^{44} variant (orange), and wild-type Ser (blue).

the NH_2-terminus of an α helix, Pro can promote stabilization of the helix because it restricts conformational freedom (*24*) but in general has low helix propensity because of the strain energy that it tends to introduce (*25*). Gly has low helix propensity because of the entropy cost associated with its backbone conformational flexibility and because it lacks hydrophobic stabilization (Fig. 2). Ala provides some hydrophobic stabilization (Fig. 2A) without incurring the entropy cost associated with the conformational restriction of a γ substituent within an α helix. For the 17 remaining amino acids, differences in the burial of hydrophobic surface seem to be most important. The agreement between substitutions at sites 44 and 131 in T4 lysozyme is stronger than the correspondence with replacements at site 32 of barnase (*9*) (correlation of 62%). However, this site is at the Ccap − 2 position (*9*), that is, within the last turn of the helix, and may not be comparable with the internal sites (Ccap − 7 and Ccap − 4) used in T4 lysozyme.

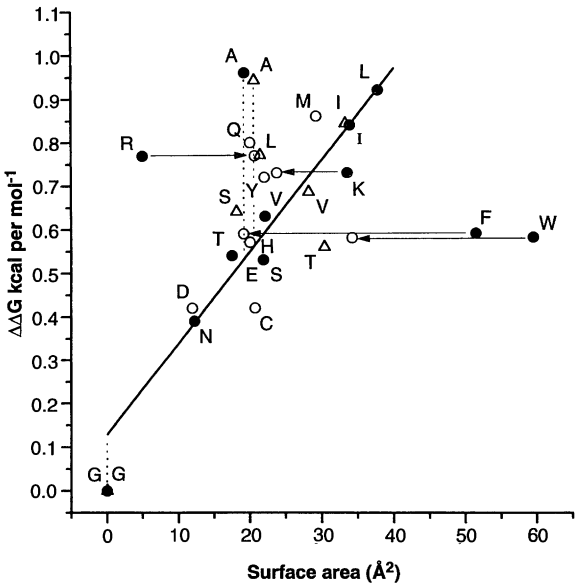

Fig. 2. Free energies of unfolding ΔΔG relative to Gly of a series of lysozymes with different amino acids substituted at site 44 of T4 lysozyme plotted against the surface area of the side chain of residue 44 that is buried during helix formation, on the basis of the available crystal structures (closed circles) (*30, 31*). Substitutions are identified by the one-letter code for amino acids (*32*). The side chain conformations of Arg^{44} and Lys^{44} are probably influenced by crystal contacts (*22*). The Phe^{44} and Trp^{44} variants crystallize in non–wild-type crystal forms with, respectively, two and four molecules per asymmetric unit. Values shown are the averages of the two- and four-crystal structures, respectively (*22*). Side chain buried areas for substitutions at site 44 for which crystal structures were not available (open circles) were calculated on the assumption that the side chain of the site 44 replacement was fully extended and the structure was otherwise identical with that of the wild type. Buried areas for substitutions at position 131 (open triangles) were calculated from observed crystal structures.

Table 1. Helix propensity values. T4L, T4 lysozyme. All free-energy scales have been normalized so that the helix propensity of Gly is 0. The symbol P_{mid} represents the relative frequency with which the amino acid occurs in the middle of α helices in known protein structures; *s* is the Zimm-Bragg parameter and the correlation is with *RT* ln*s*. The sources of data are indicated by the reference numbers at the top of their respective columns.

Amino acid	ΔΔG (kcal mol⁻¹)					Percent helix (*5*)	P_{mid} (*2*)	*s* (*3*)
	T4L site 44*	T4L site 131†	(*6*)	(*4*)	Barnase site 32 (*9*)			
Ala	0.96	0.94	0.79	0.77	0.91	78	1.41	1.07
Leu	0.92	0.77	0.62	0.62	0.56	80	1.34	1.14
Met	0.86	0.81	0.57	0.50	0.60		1.30	1.20
Ile	0.84	0.84	0.39	0.23	0.10	41	1.09	1.14
Gln	0.80		0.48	0.33	0.43		1.27	0.98
Arg	0.77			0.68	0.77		1.21	1.03
Lys	0.73			1.23	0.72		1.23	0.94
Tyr	0.72			0.17	0.09		0.74	1.02
Val	0.63	0.69	0.34	0.14	0.03	17	0.98	0.95
Phe	0.59			0.41	0.22	23	1.16	1.09
Trp	0.58			0.45	0.07		1.02	1.11
His	0.57			0.06	0.13		1.05	0.69
Thr	0.54	0.56	0.23	0.11	0.12		0.76	0.82
Glu	0.53	0.88‡		0.27	0.36		1.18	1.35
Ser	0.53	0.64	0.28	0.35	0.50		0.57	0.76
Asp	0.42	0.77‡		0.15	0.20		0.99	0.78
Cys	0.42			0.23	0.09		0.66	0.99
Asn	0.39		0.18	0.07	0.25		0.76	0.78
Gly	0.00	0	0.00	0.00	0.00		0.43	0.59
Pro§	−2.50			−3.00			0.19	0.19

*The conditions for optimal reversibility of unfolding and two-state behavior were 0.025 M KCl, 0.003 M H_3PO_4, and 0.017 M KH_2PO_4 (pH 3.01). The difference between the free energy of unfolding of each mutant and that of the Gly variant used as the reference was determined by van't Hoff analysis (*17, 33*). The estimated uncertainty in ΔΔG for all mutants is less than 0.10 kcal mol⁻¹. †Data are from (*8*) and this work. The values of ΔΔG determined under conditions identical to those used for the site 44 replacements. ‡Glu and Asp were not included in the determination of the correlation because of presumed electrostatic stabilization. §Correlations with the site 44 data from T4 lysozyme, excluding Pro: T4L site 131, 0.97, (*6*), 0.93; (*4*), 0.71; barnase site 32, 0 62; percent helix, 0.93; P_{mid}, 0.81; and *s*, 0.69.

REFERENCES AND NOTES

1. P. Y. Chou and G. D. Fasman, *Annu. Rev. Biochem.* **47**, 251 (1978).
2. R. W. Williams, A. Chang, D. Juretic, S. Loughran, *Biochim. Biophys. Acta* **916**, 200 (1987).
3. J. Wojcik, K.-H. Altmann, H. A. Scheraga, *Biopolymers* **30**, 121 (1990).
4. K. T. O'Neil and W. F. DeGrado, *Science* **250**, 646 (1990).
5. S. Padmanabhan, S. Marqusée, T. Ridgeway, T. M. Laue, R. L. Baldwin, *Nature* **344**, 268 (1990).
6. P. C. Lyu, M. I. Liff, L. A. Marky, N. R. Kallenbach, *Science* **250**, 669 (1990).
7. G. Merutka, W. Lipton, W. Shalongo, S.-H. Park, E. Stellwagen, *Biochemistry* **29**, 7511 (1990).
8. S. Dao-pin, W. A. Baase, B. W. Matthews, *Proteins Struct. Funct. Gen.* **7**, 198 (1990).
9. A. Horovitz, J. M. Matthews, A. R. Fersht, *J. Mol. Biol.* **227**, 560 (1992).
10. J. Hermans, A. G. Anderson, R. H. Yun, *Biochemistry* **31**, 5646 (1992).
11. T. P. Creamer and G. D. Rose, *Proc. Natl. Acad. Sci. U.S.A.* **89**, 5937 (1992).
12. Additional details of the site selection process will be given elsewhere (M. Blaber *et al.*, in preparation). The sequence of the α helix (positions 39 to 50) in which Ser^{44} is included is Leu-Asn-Ala-Ala-Lys-Ser-Glu-Leu-Asp-Lys-Ala-Ile. For the 12 residues in the α helix, the mean Ramachandran angles are $\phi = -67° \pm 9°$ and $\psi = -41° \pm 6°$.
13. J. W. Taylor, J. Ott, F. Eckstein, *Nucleic Acids Res.* **13**, 8765 (1985); T. A. Kunkel, J. D. Roberts, R. A. Zakour, *Methods Enzymol.* **154**, 367 (1987).
14. T. Alber and B. W. Matthews, *Methods Enzymol.* **154**, 511 (1987); D. C. Muchmore, L. P. McIntosh, C. B. Russell, D. E. Anderson, F. W. Dahlquist, *ibid.* **177**, 44 (1989); A. R. Poteete, S. Dao-pin, H. Nicholson, B. W. Matthews, *Biochemistry* **30**, 1425 (1991).
15. Presumably because Ser^{44} in crystals of wild-type lysozyme is moderately close to a crystal contact, the variants with the bulky substitutions Phe and Trp crystallized in different forms (Phe: space group $P2_1$, $a = 54.1$ Å, $b = 55.9$ Å, $c = 59.9$ Å, $\beta = 103.6°$, two molecules per asymmetric unit, resolution of 1.85 Å; Trp: space group $P1$, $a = 54.4$ Å, $b = 64.3$ Å, $c = 59.5$ Å, $\alpha = 101.1°$, $\beta = 89.9°$, $\gamma = 115.0°$, four molecules per asymmetric unit, resolution of 2.05 Å). All other variants that were crystallized were isomorphous with the wild type (resolution of 1.7 to 1.9 Å). The Glu variant gave crystals in yet another form. Diffraction data were collected (*26*) and all the structures were determined and refined to the resolution limits defined above (*R* values between 14.9 and 17.2%; bond length deviation of 0.012 to 0.019 Å; bond angle deviation of 1.9° to 2.3°).
16. The crystal structures of variants with Val, Ala, and Thr at position 131 have been reported in (*8*). Additional replacements with Asp, Gly, Ile, Leu, and Ser have been constructed, their stabilities have been measured, and their crystal structures have been determined; statistical values are com-

parable with those of the replacements at site 44. The χ^1 values of Val^{44}, Ile^{44}, and Thr^{44} are, respectively, 164°, −73°, and −66°; all are close to an expected energy minimum. It was argued on the basis of Ala, Val (χ^1 = 162°), and Thr (χ^1 = −76°) substitutions at site 131 that β branched amino acids might be helix-destabilizing because of the strain introduced, although the apparent strain energy was not large (*17*). The possible involvement of strain in such cases remains an open question.

17. X.-J. Zhang, W. A. Baase, B. W. Matthews, *Biochemistry* **30**, 2012 (1991).
18. K. A. Dill and D. Shortle, *Annu. Rev. Biochem.* **60**, 795 (1991); D. Shortle, H. S. Chan, K. A. Dill, *Protein Sci.* **1**, 201 (1992).
19. F. M. Richards and T. Richmond, *Ciba Found. Symp.* **60**, 23 (1978).
20. P. Y. Chou, M. Wells, G. D. Fasman, *Biochemistry* **11**, 3028 (1972); O. B. Ptitsyn, *Pure Appl. Chem.* **31**, 227 (1972).
21. C. Tanford, *The Hydrophobic Effect* (Wiley, New York, ed. 2, 1980); C. Chothia, *Nature* **248**, 338 (1974); F. M. Richards, *Annu. Rev. Biophys. Bioeng.* **6**, 151 (1977); R. B. Hermann, *Proc. Natl. Acad. Sci. U.S.A.* **74**, 4144 (1977); A. E. Eriksson *et al.*, *Science* **255**, 178 (1992).
22. It is expected that the helix propensity of Gly is less than that predicted from hydrophobic stabilization alone because of the increase in backbone configurational entropy associated with this amino acid (*27, 28*). (This decrease in helix propensity for Gly is indicated by the dotted vertical line in Fig. 2.) That the helix propensity of Ala is greater than that expected on the basis of hydrophobic stabilization alone (shown by the vertical dotted line in Fig. 2) can also be rationalized in terms of the lack of a γ carbon in Ala and the consequently reduced side chain configurational entropy (*8, 17, 27*). Thus, the remaining outliers are Arg, Phe, and Trp, which all have long, bulky side chains. In the crystal structure, the Arg^{44} side chain adopts an unusual (nonextended) conformation (Fig. 1A) such that two of the guanidino nitrogens form hydrogen bonds with the side chain of Asn^{116} of a neighboring molecule in the crystal lattice. (The ε amino group of Lys^{44} participates in a similar intermolecular interaction in the Lys^{44} crystal structure.) If it is assumed that the side chains of Arg^{44} and Lys^{44} adopt fully extended conformations in solution, then the estimated hydrophobic stabilization of each of these residues corresponds moderately well with its observed helix propensity (● → ○, in Fig. 2). The buried surface areas of the bulky residues Phe and Trp do not appear to correspond to their helix propensities (Fig. 2). However, in both cases there were complications in the structural analysis that might affect the calculation of surface area. The Phe^{44} variant crystallized in a form different from that of the wild type with two molecules per asymmetric unit. The Trp^{44} variant crystallized in yet another form with four molecules per asymmetric unit. All six of these mutant lysozyme molecules have Phe^{44} or Trp^{44} in the trans conformation ($\chi_1 \sim 180°$) (Fig. 1B). This conformation is the same as that of Ser^{44} in the native protein but is different from all the other position-44 variants, which are gauche$^+$ ($\chi_1 \sim -60°$). Because they adopt the trans conformation, Phe^{44} and Trp^{44} are close to Glu^{45} and to Lys^{48} in the next turn of the α helix. This proximity helps to explain why the calculated buried surface area of Phe^{44} and Trp^{44} is so much larger than that of the other position-44 replacements (Fig. 2). On the other hand, the contacts between either Trp^{44} or Phe^{44} and residues 45 and 48 are tenuous. In the crystal structures of these variants, there are on average only 2.6 van der Waals contacts of less than 3.5 Å between any side chain atom in residue 44 and any side chain atom in residues 45 and 48. On the assumption that in solution Glu^{45} and Lys^{48} do not reduce the solvent-accessible areas of Phe^{44} and Trp^{44}, the hydrocarbon surface area that these two residues would then bury is close to their observed hydrophobic stabilization (● → ○ in Fig. 2).

23. M. J. McGregor, S. A. Islam, M. J. E. Sternberg, *J. Mol. Biol.* **198**, 775 (1987).
24. H. Nicholson, D. E. Tronrud, W. J. Becktel, B. W. Matthews, *Biopolymers* **32**, 1431 (1992).
25. U. H. Sauer, S. Dao-pin, B. W. Matthews, *J. Biol. Chem.* **267**, 2393 (1992).
26. M. G. Rossmann, *J. Appl. Crystallogr.* **12**, 225 (1979); M. F. Schmid *et al.*, *Acta Crystallogr. A* **37**, 701 (1981); R. Hamlin, *Methods Enzymol.* **114**, 416 (1985).
27. G. Nemethy, S. J. Leach, H. A. Scheraga, *J. Phys. Chem.* **70**, 998 (1966).
28. B. W. Matthews, H. Nicholson, W. J. Becktel, *Proc. Natl. Acad. Sci. U.S.A.* **84**, 6663 (1987).
29. B. Lee and F. M. Richards, *J. Mol. Biol.* **55**, 379 (1971).
30. The buried area was determined as the difference between the folded and the unfolded solvent-accessible surfaces (*29*) of the residue 44 side chain. The unfolded state for each mutant was modeled by a fully extended tripeptide (φ = −139°, ψ = 135°) (*19*) with the same sequence (Lys-X-Glu) as residues 43 to 45. The side chain at site 44 was taken to be fully extended and the calculated solvent accessibility was taken as the average of the values for the gauche$^+$, gauche$^-$, and trans conformations. For each mutant, the folded protein was taken as the protein that was observed in the respective crystal structure. Only the hydrocarbon surface area (all carbon atoms plus S^γ of Met) was included in the calculation. The radius of the probe used for the calculations was 1.4 Å. The straight line was fitted by linear regression to the points for Asn, Glu, Ser, Thr, Val, Lys, Ile, and Leu (correlation coefficient = 0.96).
31. The solvent-accessible surface area that is buried upon helix formation should be small (less than that of a methyl group) and the corresponding hydrophobic stabilization is also small (less than 1 kcal mol^{-1}). Estimates of buried surface area are therefore sensitive to changes in side chain conformation, geometry of the α helix, and the model used in the estimation of the solvent-exposed area in the unfolded state. In an attempt to minimize these sources of uncertainty, we based the surface area calculation only on the side chains of the substituted residue. Calculations of surface area based on the helix as a whole, as well as attempts to estimate entropic effects, will be described elsewhere (M. Blaber *et al.*, in preparation).
32. Abbreviations: A, Ala; C, Cys; D, Asp; E, Glu; F, Phe; G, Gly; H, His; I, Ile; K, Lys; L, Leu; M, Met; N, Asn; Q, Gln; R, Arg; S, Ser; T, Thr; V, Val; W, Trp; Y, Tyr.
33. W. J. Becktel and J A. Schellman, *Biopolymers* **26**, 1859 (1987).
34. We thank S. Pepiot and J. Wozniak for help with purifying the mutant lysozymes, G. D. Rose and F. M. Richards for helpful comments on the manuscript, and J. Lindstrom and W. A. Baase for determining the thermodynamic parameters. Supported by grants from the National Institutes of Health (GM 21967) and the Lucille P. Markey Charitable Trust.

16 December 1992, accepted 9 April 1993

A Nonpeptidyl Growth Hormone Secretagogue

Roy G. Smith,* Kang Cheng, William R. Schoen, Sheng-Shung Pong, Gerard Hickey, Tom Jacks, Bridget Butler, Wanda W.-S. Chan, Lee-Yuh P. Chaung, Fred Judith, Joyce Taylor, Matthew J. Wyvratt, Michael H. Fisher

A nonpeptidyl secretagogue for growth hormone of the structure 3-amino-3-methyl-*N*-(2,3,4,5-tetrahydro-2-oxo-1-{[2′-(1*H*-tetrazol-5-yl)(1,1′-biphenyl)-4-yl]methyl}-1*H*-1-benzazepin-3(*R*)-yl)-butanamide (L-692,429) has been identified. L-692,429 synergizes with the natural growth hormone secretagogue growth hormone–releasing hormone and acts through an alternative signal transduction pathway. The mechanism of action of L-692,429 and studies with peptidyl and nonpeptidyl antagonists suggest that this molecule is a mimic of the growth hormone–releasing hexapeptide His-D-Trp-Ala-Trp-D-Phe-Lys-NH_2 (GHRP-6). L-692,429 is an example of a nonpeptidyl specific secretagogue for growth hormone.

The availability of recombinant human growth hormone (GH) has resulted in renewed interest in GH therapy. Aging is associated with an attenuation of the amplitude and frequency of pulsatile GH release; by age 40, a reduced responsiveness of the pituitary gland to GH-releasing hormone (GRF) is evident (*1*). GH replacement therapy may reverse some of the bodily changes associated with aging (*2*); thus, GH treatment may prove beneficial to the elderly. In addition to its utility in the treatment of GH-deficient children, GH accelerates healing of severely burned children (*3*), is beneficial in preventing catabolic side effects in patients treated with prednisone (*4*), acts as an adjuvant to gonadotrophin treatment for ovulation induction (*5*), may prevent osteoporosis (*6*), and improves exercise capacity in GH-deficient adults (*7*). GH also stimulates T cell development, which suggests that it may be useful for the treatment of T cell deficiencies (*8*).

Current methods of treating GH deficiency are not ideal. GH, a large polypeptide, lacks oral bioavailability, and injection results in prolonged elevation of GH

R. G. Smith, K. Cheng, S.-S. Pong, G. Hickey, T. Jacks, B. Butler, W. W.-S. Chan, L.-Y. P. Chaung, F. Judith, J. Taylor, Department of Basic Animal Science Research, Merck Research Laboratories, Rahway, NJ 07065.
W. R. Schoen, M. J. Wyvratt, M. H. Fisher, Department of Basic Medicinal Chemistry, Merck Research Laboratories, Rahway, NJ 07065.

*To whom correspondence should be addressed.